The Structural Design of Tall and Special Buildings

WILEY

RESEARCH ARTICLE OPEN ACCESS

Robustness of Dry-Assembled Precast Wall and Coupled Wall-Frame High-Rise Structures With Voided Prestressed Slabs

Bruno Dal Lago[1] | Krunal Gajera[2] | Paolo Martinelli[3]

[1]Department of Theoretical and Applied Sciences, Università degli Studi dell'Insubria, Varese, Italy | [2]DLC Consulting srl, Milan, Italy | [3]Department of Civil and Environmental Engineering, Politecnico di Milano, Milan, Italy

Correspondence: Bruno Dal Lago (bruno.dallago@uninsubria.it)

Received: 3 April 2024 | **Revised:** 18 August 2024 | **Accepted:** 20 September 2024

Funding: This work was supported by the Brusnika L.l.c. company.

Keywords: high-rise buildings | mechanical connections | precast concrete | progressive collapse | risk analysis | robustness

ABSTRACT

Precast concrete structures are recognized among the structural typologies that may mostly suffer from progressive collapse as a consequence of local unpredicted damage, also due to past accidents occurred in buildings employing old precast technologies neglecting the basic robustness criteria and characterized by poorly detailed and/or executed joints and connections. Although vertical ties may relatively easily be provided in both frame and wall panel structures by employing ductile connection devices, dry-assembled precast systems avoiding concrete pouring in the whole superstructure typically struggle to provide horizontal ties as strong as required by the current standards concerning progressive collapse, in which they are not fully framed yet. Nevertheless, these systems may exploit alternative sources of robustness to stop collapse progression arising from their structural arrangement, the shape of the slab elements employed, and the slab mechanical connections. This article presents the results of a numerical investigation focused on the structural behavior of a dry-assembled precast floor system consisting of prestressed box-section slab elements employed in either wall panel or coupled wall-frame structural systems following the loss of one or multiple primary load-bearing vertical elements. Nonlinear static simulations of different loss scenarios occurring in prototypes of 100-m-tall high-rise buildings were carried out based upon spread plasticity modeling of the structural elements and experimentally calibrated nonlinear behavior of mechanical connections.

1 | Introduction

There is growing interest by the technical/scientific community in the risk for structural safety associated with difficultly predictable events with a low probability of occurrence, such as vehicle impacts, explosions, terrorist attacks, and unplanned structural alterations. These events could cause local failure of one of the vertical load-bearing elements, which could lead to successive collapse of other load-bearing elements, triggering the global chain failure phenomenon known as progressive collapse [1–3]. A recent example of progressive collapse occurred on June 24, 2021, in Surfside, a suburb of Miami (Florida, USA). The Champlain Towers South Condominium, a 12/13-storey reinforced concrete (RC) flat plate structure designed and built in 1981, experienced sudden partial collapse, causing the death of 98 people [4]. In the initial investigation of the collapse of this building, several potential causes were identified, such as differential foundation settlement, rebar corrosion, concrete cracking, and long-term waterproofing problems. The growing interest in the prevention of progressive collapse in structures is also recognized by the establishment of a specific working group (WG)

on the structural robustness for the drafting of the second generation of Eurocodes (i.e., CEN/TC 250/WG6 Robustness) and by the establishment of the "fib Action Group Robustness" for the drafting of a specific chapter on robustness to be included in the next *fib* Model Code 2020.

The ability of the structure to sustain local damage relies upon the residual capacity of the structure to redistribute gravity loads among the near undamaged elements, ensuring alternative load paths (ALP). Robustness is a fundamental characteristic for tall buildings to prevent progressive collapse or disproportionate consequences once an extreme event occurs.

Precast concrete structures are recognized among the structural typologies that may mostly suffer from the progressive collapse phenomenon due to past accidents occurred in buildings constructed employing old precast technologies that neglect robustness criteria and are characterized by poorly detailed and/or poorly executed connections and joints [5–10]. Considering cast-in-situ RC buildings, several tests have shown that the primary resistance mechanisms to column loss in frame structures are compressive arch and/or membrane actions in beams and slabs under moderate displacement, as well as tensile catenary/membrane action under large displacement [11–23]. To replicate a resistance mechanism similar to that of cast-in-situ structures, ordinary precast structures are typically constructed with topping over hollow core or double-T slab elements employing cast-in-situ pouring. Further testing showed that wet-completed precast beams and slab systems could provide substantial compressive arch action and compressive membrane action, similar to cast-in-situ RC buildings [24–37]. However, concrete topping pouring precludes many benefits of the industrial prefabrication of structural elements, and alternative solutions employing dry or semidry (completed with a small volume of mortar pouring) connection systems for all structural elements, including slabs, are currently being developed [38–40]. These floors may exploit nontraditional sources of robustness to stop collapse progression in case a primary structural element is partly or fully lost [41]. These sources are related to both the mechanical connections and the large bending and torsional strength and stiffness of the precast slab elements.

Most of the numerical and experimental studies concerning the progressive collapse of prefabricated structures (or portions of the structure) analyze frame structures [24–37, 42, 43], and wall and coupled wall-frame systems employed for mid- and high-rise buildings are rarely studied. This study focuses on the robustness of dry-assembled precast wall and coupled wall-frame high-rise structures with voided prestressed slabs. Section 2 presents the two precast systems under study, and Section 3 reports the risk analysis conducted for the buildings. Numerical finite element models are described in Section 4. The numerical investigation aims to study the behavior of these high-rise residential building typologies following the loss of one or multiple primary load-bearing vertical elements. Nonlinear static analyses are employed to simulate the most stressed parts of the structural assembly after wall/column element removal occurs at different stories. Results are presented and critically discussed in Section 5. Finally, Section 6 presents the main conclusions.

2 | Precast Systems Under Study

Slabs based on box-section elements with lower flat flange are currently employed in precast systems based on either wall panels [44] or frames [45]. Exploded images of the complete precast systems studied are shown in Figure 1, where the main analyzed elements are indicated. In the wall panel structural system, voided box prestressed slab elements with flat lower flange are mounted directly over corbels protruding from the wall panels. The load-bearing wall panels are often configured as portals due to the need for internal building distribution in the apartments/offices. Load-bearing external wall panels are provided with insulation and façade layers, alternatively to non-load-bearing RC sandwich cladding panels. Additional elements, such as stair ramps, stair landings, and balcony slabs. complete the construction. In the wall-frame structural system, similar voided box prestressed slab elements with flat lower flange are installed over the lower edge corbels of inverted-T prestressed beams. The beams are installed over square column elements. Special prestressed solid slab members are installed in correspondence of the columns in the direction of the slab to form an effective frame effect along both horizontal directions. Bracing wall panels are strongly horizontally connected with selected

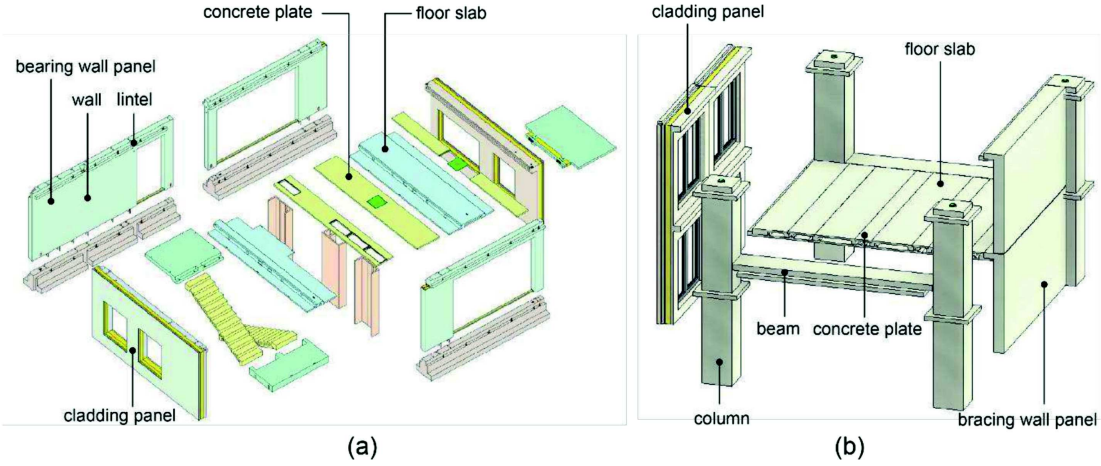

FIGURE 1 | Generic components of the precast systems under study: (a) wall and (b) coupled wall-frame.

central columns to form bracing cores. Non-load-bearing insulated sandwich RC panels clad the building perimeter. In both cases, the ceiling is fully flat due to the adoption of Gerber saddle joints in the horizontal elements, as well as the floor due to the installation of concrete plates over corner recesses left at the edges of the top flange of the slab elements. Mechanical–electrical–plumbing (MEP) systems are distributed inside the depth of the floor, avoiding further thickening above the slab.

Two similar 34-storey rectangular-plan buildings approximately 100 m high with a square structural modulus with side of 6.9 m (Figure 2) were selected as case studies. In the wall-frame building, structural bracing wall panels surround the central stair/elevator core. The structures of these buildings were fully proportioned (including reinforcement details) according to standard static and dynamic load combinations and conditions. Briefly resuming the main design data, the structures were designed following a dead nonstructural load of $2\,kN/m^2$, a live load of $2\,kN/m^2$ (doubled in common and distributive areas), a top equivalent static wind load of $1\,kN/m^2$, a seismic loading with rather low peak ground acceleration (PGA) of 0.05 g assuming elastic behavior, and acceleration induced by vortex shedding [46]. A construction stage analysis was carried out. Moreover, the building structures were also designed for robustness in the framework of a qualitative risk analysis following the approach currently suggested

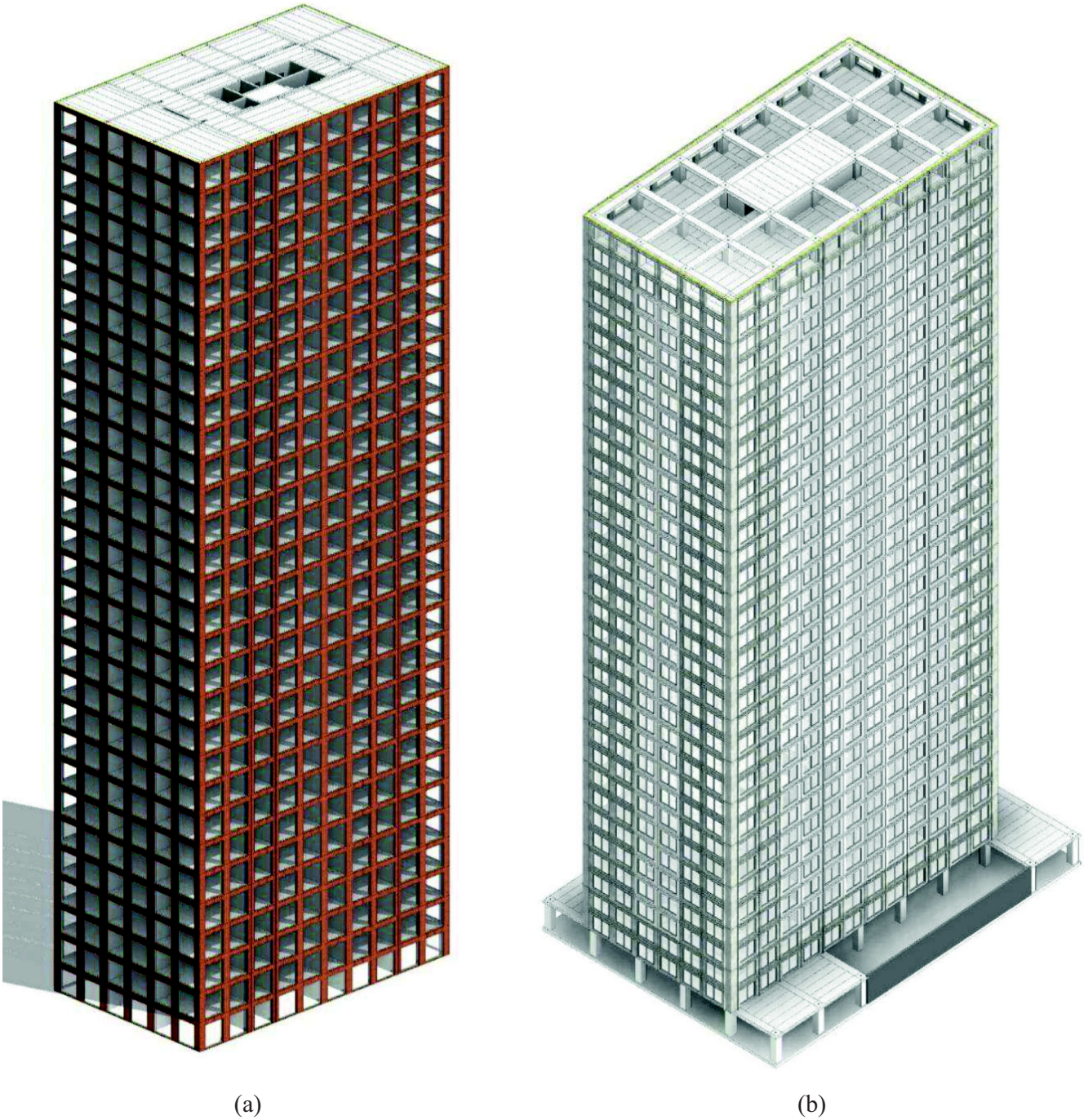

FIGURE 2 | Case study of 100-m-tall buildings: (a) wall system and (b) coupled wall-frame.

by standards. This condition, as described in the following, impacted the structural design in terms of reinforcement and connection details.

All slab elements are connected at each end to the supporting structure (either wall panel or beam) with two spaced cast-in M20 dowels, one per rib. After the dowel threaded bar is screwed into a standard coupler cast into the portal edge corbel and anchored in it through nuts and washers, the slab element is leaned over the corbels, and high-strength nonshrinking mortar is cast into the cylindric recess left by a metallic pipe. More details and shop drawings of this joint are collected in [47]. The slab elements are also mutually connected through several connections made by welding short rebar pieces to inclined steel angles anchored in the lower flange edges by means of a welded U-bent rebar. More details and shop drawings of this joint are collected in [48].

Wall panels are produced monolithically and rigidly connected with adjacent panels (wall system) or columns (coupled wall-frame system) through shear keyed vertical joints reinforced with a vertical rebar inserted in a series of consecutive flexible loops made with high-strength steel ropes protruding from both panel sides. The joint is then filled with high-strength nonshrinking cementitious mortar. More details and shop drawings of this joint are collected in [49]. The beam–column joints of the frame system are characterized by the presence of moment-resisting mechanical reinforcement couplers [50, 51] exclusively for robustness. The vertical joints of both the wall panel and frame systems are considered fully emulative due to the use of ductile mechanical rebar couplers [50, 51].

Both the horizontal and vertical elements are assumed to have similar reinforcements and cross-sections at all the storeys. This hypothesis is also assumed for the sake of simplicity of the structural model, although it could be overcome by structural optimization also taking into account the outcome of both progressive collapse and earthquake analysis, which indeed suggests that no dramatic reduction in stiffness and strength should be achieved through the different storeys (e.g., due to higher mode effects for seismic excitation).

3 | Risk Analysis

A qualitative risk analysis indicating the potential of occurrence of different hazard scenarios and the related consequences was carried out following the technical literature contained in [52–54].

The buildings under study are classified as consequence class 3 buildings (high consequences of failure) according to EN 1991-1-7 [52], which requires a systematic risk assessment. The objectives of the approach to design against disproportionate collapse based on systematic risk assessment are (i) to identify the hazards to which the structure might reasonably be subjected; (ii), so far as reasonably practicable, to eliminate the hazards that give rise to the risks; and (iii), for the hazards that remain, to develop risk reduction measures that reduce the risks arising from each hazard so far as it is reasonably practicable to do so and, in so doing, to develop a structural design that exhibits a level of structural robustness equivalent to the level of risk to which the building is subjected.

The hazard classification was considered as per Table 1, where the general hazard classification was modified to fit the precast construction systems at study, particularly by differentiating the large number of joints and mechanical connections among the elements, introducing a distinction between joints of limited (e.g., floor-to-floor), moderate (e.g., stair ramp-to-landing slab), and critical (e.g., joints between bearing vertical elements) importance, associated with the consequences of their damage or collapse.

After assumptions of effective communication among all figures involved in the construction and maintenance of the building, proper allocation to expert teams of delicate operations, design following advanced techniques by skilled design teams, and severe quality control of materials and elements produced in the precast factory, the associated hazards nos. (2), (3), (7), and (8), respectively, can be neglected.

Concerning the remaining hazards, the risk matrix shown in Figure 3 was compiled on a qualitative basis considering the specificity of both precast systems in the study, assuming that there is a negligible risk difference between them.

Furthermore, those hazards falling beyond the acceptance line are mitigated following either a reduced occurrence likelihood or reduced consequence on the building, following the risk reduction measures listed in Table 2. The new allocation of those hazards in the risk matrix of Figure 3 is shown with underlined numbers from the previous position, marked in red and barred.

The consequences of most hazards are mitigated by the adoption of the robustness criterion when designing and assembling the structure. Indeed, no systematic risk assessment can be considered a replacement for the lack of a robust structural form because no elimination of hazards can be considered fully complete to exclude any possible unpredictable scenario. For this reason, further study is needed to check the compliance of the robustness offered by the considered precast systems with normative requirements.

Compliance with general factors influencing structural robustness is analyzed in the following section. In particular, they are (I) ductility; (II) redundancy; (III) tying system; and (IV) key elements.

The ductility requirement (I) is fully checked because each main structural element of either the gravity or lateral load resisting system is provided with ductile joints due to the adoption of ductile mechanical connection devices.

The requirement (II) of redundancy is generally only partially checked in dry-assembled precast structures because many joints are designed as hinges. However, as pointed out by the analysis shown in the following, this condition may be considered checked because the structure is able to track ALP after removal of a main load-bearing element.

The tying requirement (III) is also checked, although in a nonconventional way. In particular, both wall-frame and wall panel systems are conceived with ductile vertical connections that ensure the continuity and ductility of the vertical

TABLE 1 | Hazard classification.

	Hazard ID	Hazard
Organizational factors	(1)	Structural risk management error
	(2)	Communication and collaboration
	(3)	Allocation of responsibilities
	(4)	Safety culture
Design phase	(5)	Numerical and conceptual mistake in analysis or design
	(6)	Incorrect dimensioning on drawings or conflicting/missing drawings or calculations
	(7)	Designing with (new) methods or techniques which turnout not to behave as predicted
Production phase	(8)	Substandard elements and components
	(9)	Inadequate concrete strength for demolding, application of prestressing, or lifting
Assembly phase	(10)	Improper assemblage, tightening, welding, or grouting of the joint/connection
	(10a)	Joints of limited importance
	(10b)	Joints of moderate importance
	(10c)	Joints of critical importance
During use	(11)	Insufficient maintenance
	(12)	Occurrence of unforeseeable natural hazard (earthquake, landslide, hurricane, and snowstorm)
	(13)	Fire
	(14)	Explosion (gas leak, dust or chemical, bomb, and excavation blast)
	(15)	Impact by vehicle (car/truck)
	(16)	Unplanned future alteration
	(17)	Change in soil condition
	(18)	Excavation, sink holes, slides, etc., in the neighborhood

reinforcement from the foundation. The slab systems are also provided with different types of horizontal ties. In the wall panel system, the main horizontal ties are provided by the joints between wall portals, and the secondary horizontal ties are provided by the slab elements through dowel slab-to-wall and welded slab-to-slab connections. In the wall-frame system, the main horizontal ties are provided by the emulative joint columns and either the beam, tragolo, or special slab, and the secondary horizontal ties are provided by the slab elements through dowel slab-to-wall and welded slab-to-slab connections. Notably, the single slab-to-slab welded connections provide a strength lower than the requirement of the specific part of Eurocode 1 [52] for single ties. Nevertheless, the number of welded connections can be easily determined to fulfill the requirements of several distributed ties. In both systems, peripheral ties are always provided through horizontal reinforcement of all peripheral elements and dowel connections of the cladding panel elements.

Finally, the requirement (IV) of key elements, as defined in EN 1991-1-7 [52], can be easily fulfilled by designing every main structural element to avoid suffering from severe damage after a reasonable blast or impact loading due to their dimensions and capacity.

4 | Numerical Modeling Strategy for Notional Removal of Main Elements

The approach to designing for unspecified hazards involves a notional damage scenario method. According to the current draft version of the *fib* Model Code 2020 document [55], this

RISK MATRIX		Consequence						
		Minimal	Minor	Significant	Serious	Substantial	Severe	Catastrophic
Likelihood	Frequent/common	~~(9)~~						
	Likely	(9)	~~(1)~~-(4)-(11)-(16)-(18)	~~(16)~~				
	Unlikely	(10a)	(1)-(10b)-(17)		~~(5)~~			
	Rare		(13)-(15)	(10c)-~~(13)~~-~~(15)~~	(5)-~~(6)~~			
	Improbable			(14)	(6)	(12)	~~(12)~~	
	Negligible							

FIGURE 3 | Risk matrix. The acceptance threshold is indicated by the bolded line. Deleted red hazards are replaced by underlined hazards in the new position after risk reduction measures are taken.

TABLE 2 | Risk reduction measures.

Hazard ID	Risk reduction measure	Cost	Benefit
(1)	Deeper analysis	+	Reduced likelihood
(5)	Additional design team and checks	+	Reduced likelihood
(6)	Additional design team and checks	+	Reduced likelihood
(9)	Discarding of flawed elements	+(+)	Reduced likelihood
(12)	Wider design scenarios and improved structural robustness	+(++)	Reduced consequence
(13)	Wider design scenarios and implementation of active fire extinction systems	++(+)	Reduced consequence
(15)	Impact design of outdoor area	+(+)	Reduced consequence
(16)	Careful design of future alteration internal to the company	+	Reduced consequence

method encompasses two possible approaches: notional deterioration scenarios and notional element-removal scenarios. In the former, the geometric or material properties of one or more structural elements are reduced (see, e.g., [56, 57]), whereas in the latter, structural elements are removed. In both cases, the structural safety of the modified structure is then assessed to ensure its ability to provide an ALP for the imposed loads. Among the structural elements subjected to hypothetical removal, columns (one or more) and panels/walls (one or more) are the most considered. The notional removal scenario strategy is applied in this study. This approach has been widely used in the research literature to evaluate the robustness of buildings, as exemplified by studies such as those of Ravasini et al. [29] and Martinelli et al. [22], among others. It should be noted that the notional removal scenario approach adopted here is more conservative than the notional deterioration scenario approach.

Portions of the case study buildings were selected as indicated in Figure 4 by a red rectangle for the notional removal of the main vertical load-bearing elements. These structural portions were selected to be representative of the areas most stressed after notional removal. The main cross sections and longitudinal reinforcements of the primary structural elements modeled nonlinearly are shown in Figure 5.

The general-purpose finite element code Straus7 [58] was employed for modeling with the strategies described in Figure 6. The beams/lintels and columns/walls were modeled with nonlinear beam elements to which the distributed plasticity was attributed through nonlinear moment–curvature diagrams integrated by the software within embedded Gauss–Lobatto points. The physical encumbrance of the joint areas was modeled with rigid beam or link elements. On the basis of a concrete class C40/50 modeled in compression with a Sargin/Saenz constitutive law [59] (Figure 7a), for which the tensile strength was neglected, and of a reinforcing steel class B450C modeled with a linear-parabolic model (Figure 7b), nonlinear moment–curvature diagrams were obtained, as partially shown in Figure 8, with few representative cross sections subjected to different axial loads. Nonlinear sectional properties were obtained on the basis of nominal characteristic material strength properties for concrete, steel, and connections (where experimental data were not used), following the common approach under accidental loading combinations (fire, blast, and impact). Trilinearization of the resulting nonlinear diagrams in both main and transverse bending was carried out, as requested by the software input [58]. The slab elements were modeled with elastic shell elements. Floor connections were modeled with nonlinear springs to which the

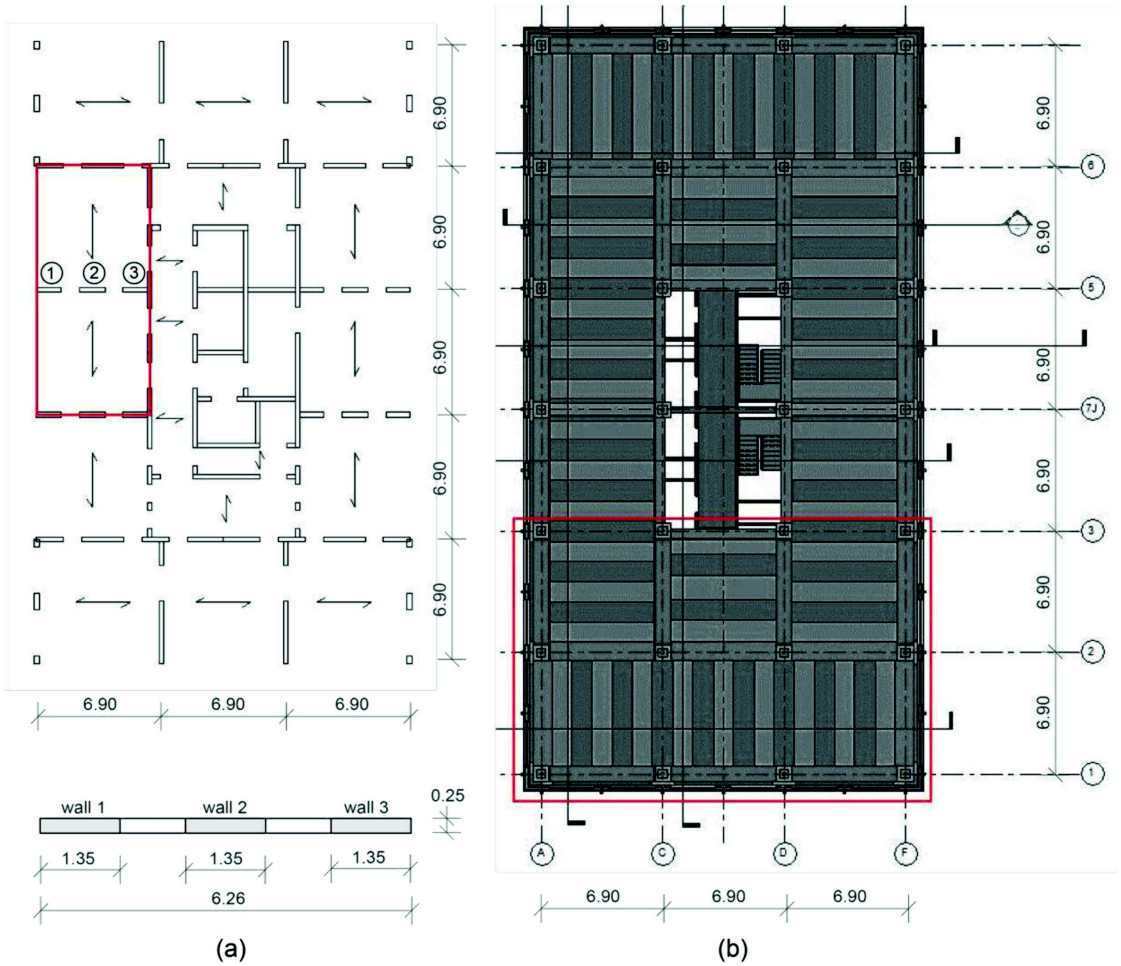

FIGURE 4 | Plant area modeled and analyzed for (a) wall system and (b) coupled wall-frame (unit: m).

force–displacement diagrams were attributed following the trilinearization of the experimental data, some of which (confined M20 slab dowel in shear [47]; confined M20 slab dowel in tension; corbel under localized compression; welded-bar angle connection [48]) carried out with original testing instrumental for the present analysis, as shown in Figure 9.

The applied loads other than the self-weight of the structural elements, automatically computed, are the nonstructural dead load (2.0 kN/m^2), live load associated with residential use (2.0 kN/m^2 becoming 0.6 kN/m^2 in the proper combination), and precast concrete cladding panel load (6.0 kN/m—50% glazing).

Rigid diaphragm behavior was considered for the surrounding building portions not explicitly included in the model because of the presence of the slab mechanical connections, as also experimentally assessed in [60].

5 | Analysis and Discussion

Static nonlinear pushdown analyses including both mechanical and geometrical nonlinearities were carried out considering different scenarios of column/wall loss, encompassing loss of a single wall element or multiple wall elements part of the same considered panel of the wall system, and loss of different columns (internal, edge, and corner) for the coupled wall-frame system. The loss scenario was considered at different positions along the height of the tower buildings, from the ground to the roof storeys. The analyses were carried out under load control by progressively increasing the load up to 100% of the load associated with the accidental combination [52] by subdividing it in 10 subincrements. The software then automatically further subdivides the calculation steps by maximum 10 times until convergence occurs, according to a displacement norm tolerance of 10^{-4} m. Divergence is classified after the convergence criterion described above is not attained after 50 iterations at the narrower substep. The consequences of the notional removal of the primary element(s) from the model are supposed not to depend on the dynamic response of the structure, which is indeed deemed to be a reasonable assumption, because even after an impact or blast event, it is unlikely that bulk solid heavily RC columns/walls strongly connected with the surrounding elements and characterized by a low aspect ratio completely disappear in fractions of a second [61]; therefore, a progressive failure in the quasistatic strain rate range is employed to indirectly simulate a relatively slow complete loss of stiffness and strength of the element under removal.

Table 3 shows the main results of all the static nonlinear analyses carried out. In particular, the model ID identifies the type of precast system (WA, wall; or WF, coupled wall-frame), the storey at

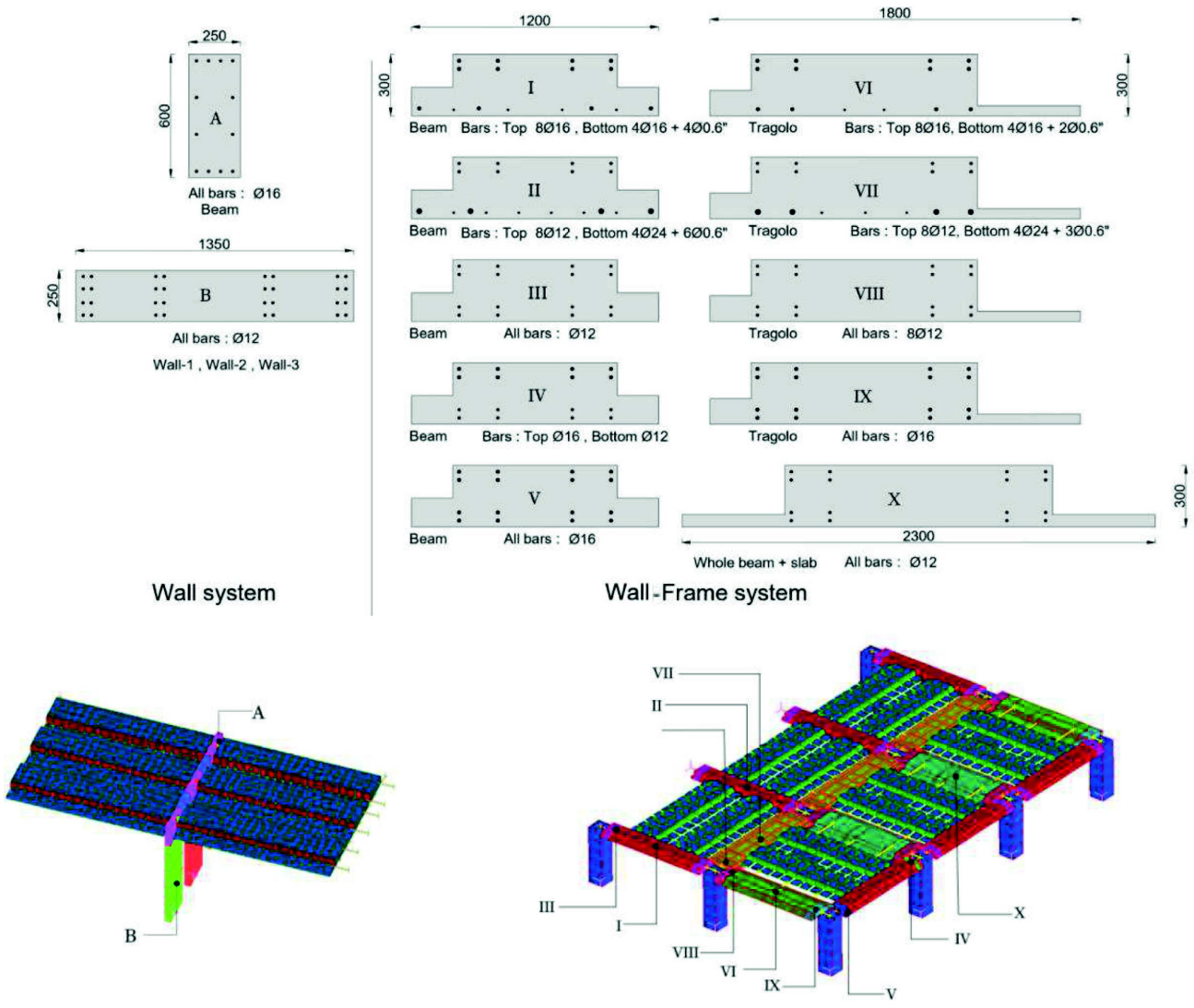

FIGURE 5 | Cross sections of the primary structural elements: (a) wall system and (b) coupled wall-frame system.

which a primary element is removed (from the top [34th storey] to the ground [1st storey]), and the considered scenario (for the wall system, the numbers indicate the contemporary removal of wall portions 1, 1&2, and 1&2&3, as indicated in Figure 4a; for the coupled wall-frame system, the number and letter identify the single column removed, referring to the grid of Figure 4b).

5.1 | Wall System

It was observed that the loss of a single wall in a typical three-wall panel yields a structural behavior of the surrounding structural elements remaining in the elastic field regardless of the storey at which collapse occurs, which is mainly a consequence of the high stiffness and strength of the lintel element. The contemporary loss of two or even three walls in a single three-wall panel imposes tougher conditions on the structure, with plasticization of the lintel and a complex distribution of loads in the slab elements and connections. Two resistance mechanisms—(1) the frame action of the elements above acting in bending/shear and (2) the torque action of the slab system—work in parallel and are independent sources of structural robustness for the considered precast system.

In the case of the loss of walls 1 and 2 at the roof storey, without the additional elements above being able to activate the frame contribution, the torsional stiffness and strength of the slab elements and their connections are the only sources of mitigation of the bending moment distribution on the lintel. Figure 10a shows the elastic bending moment distribution over the lintel element modeled alone, thus not accounting for the slab contribution. The maximum moment acting on the lintel element outside of the wall physical area is 740 kNm, which is more than double the lintel bending strength (Figure 8); thus, this analysis is far from checked. A possible equilibrium condition could not be found even by catenary action because the isolated lintel element is restrained with a cantilever scheme that is statically determined in both the transverse and longitudinal directions.

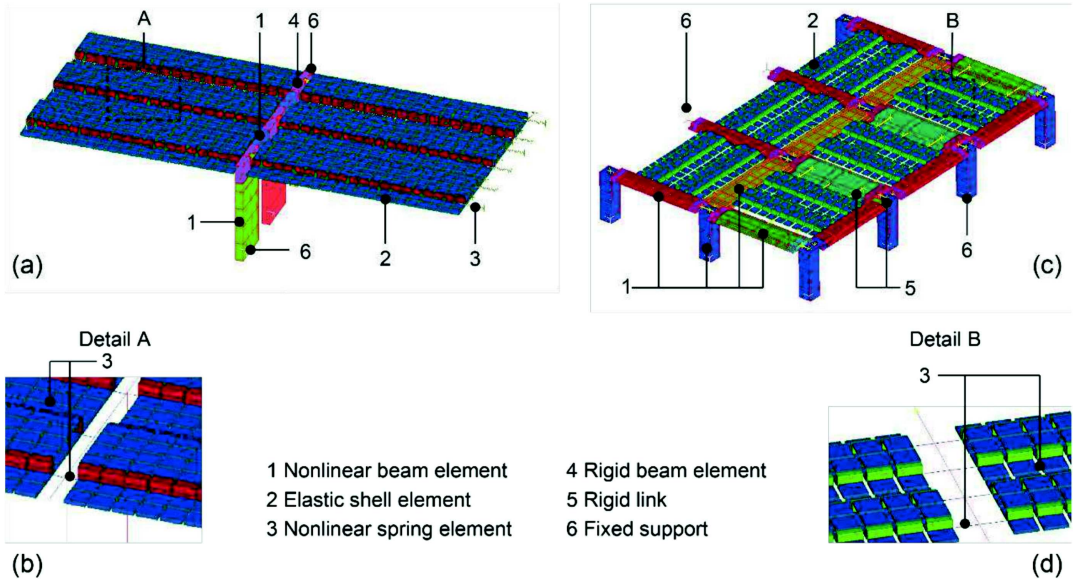

FIGURE 6 | Numerical models: (a) picture of the wall system model (ground floor), (b) element details of the wall system model, (c) picture of the coupled wall-frame system model (ground floor), and (d) element details of the coupled wall-frame system model.

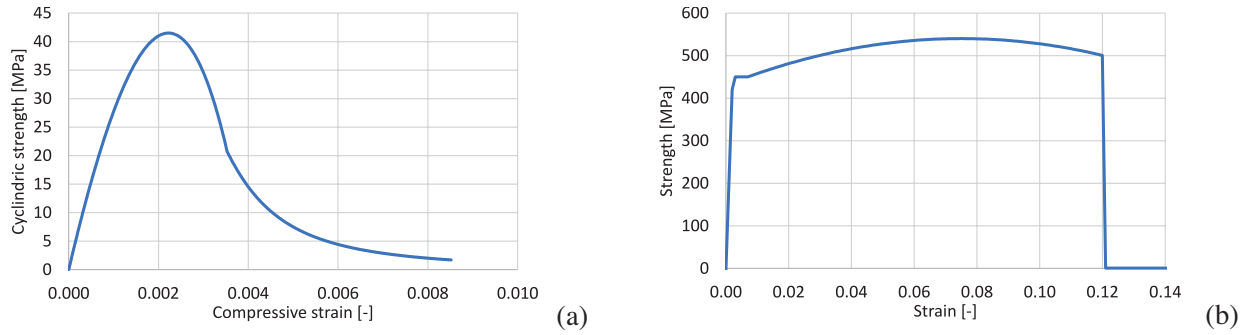

FIGURE 7 | Constitutive laws for the materials employed. (a) Sargin/Saenz model for concrete C40/50. (b) Elastic–parabolic model for steel class B450C.

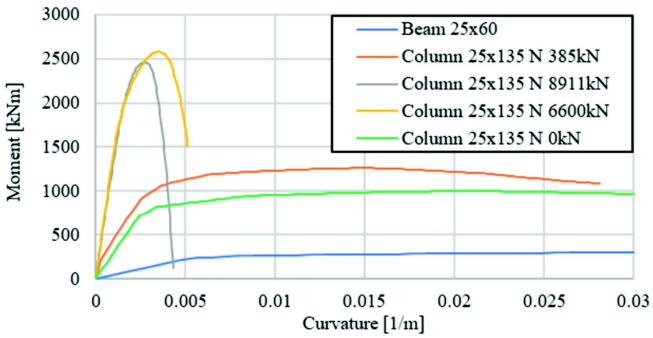

FIGURE 8 | Nonlinear moment–curvature diagrams for beam (lintel) and column (wall) elements of the precast wall panel system with different axial load (N) values.

When introducing nonlinearities in the model and the presence of the slab, the diagram is modified according to Figure 10b, where the bending moment in the critical section decreases to 338 kNm, which is compatible with the plasticized state of the lintel, due to the introduction of warping couples concentrated in correspondence with the slab ribs, as shown in Figure 10c, which is attributed to the torque stiffness of the box core of the slab element. The maximum actions on the slab connections appear compatible with the strengths associated with both slab-to-lintel dowel and slab-to-slab welded connections. In particular, the torsional effect of the slab was exhibited by the warp coupling of the vertical actions displayed in the dowel connections corresponding to the ribs. These forces, combined with the downward gravity actions, occur together with shear actions in both horizontal directions, leading to complex interactions. However, owing to the detailing of the dowel connection, the combination of these actions appears to be compatible with the strength of the dowel, corbel, and welded connections obtained by experimentation. The displacements obtained in the analyses, limited to a few centimeters for the analysis WA-34-12 (Figure 11a), are much smaller than those traditionally associated with large displacement second-order effects such as one-way catenary or two-way tensile membrane action (TMA), thus making the studied precast systems much less vulnerable (and easily repairable) than more traditional cast-in-situ and precast RC systems under the scenario of wall losses.

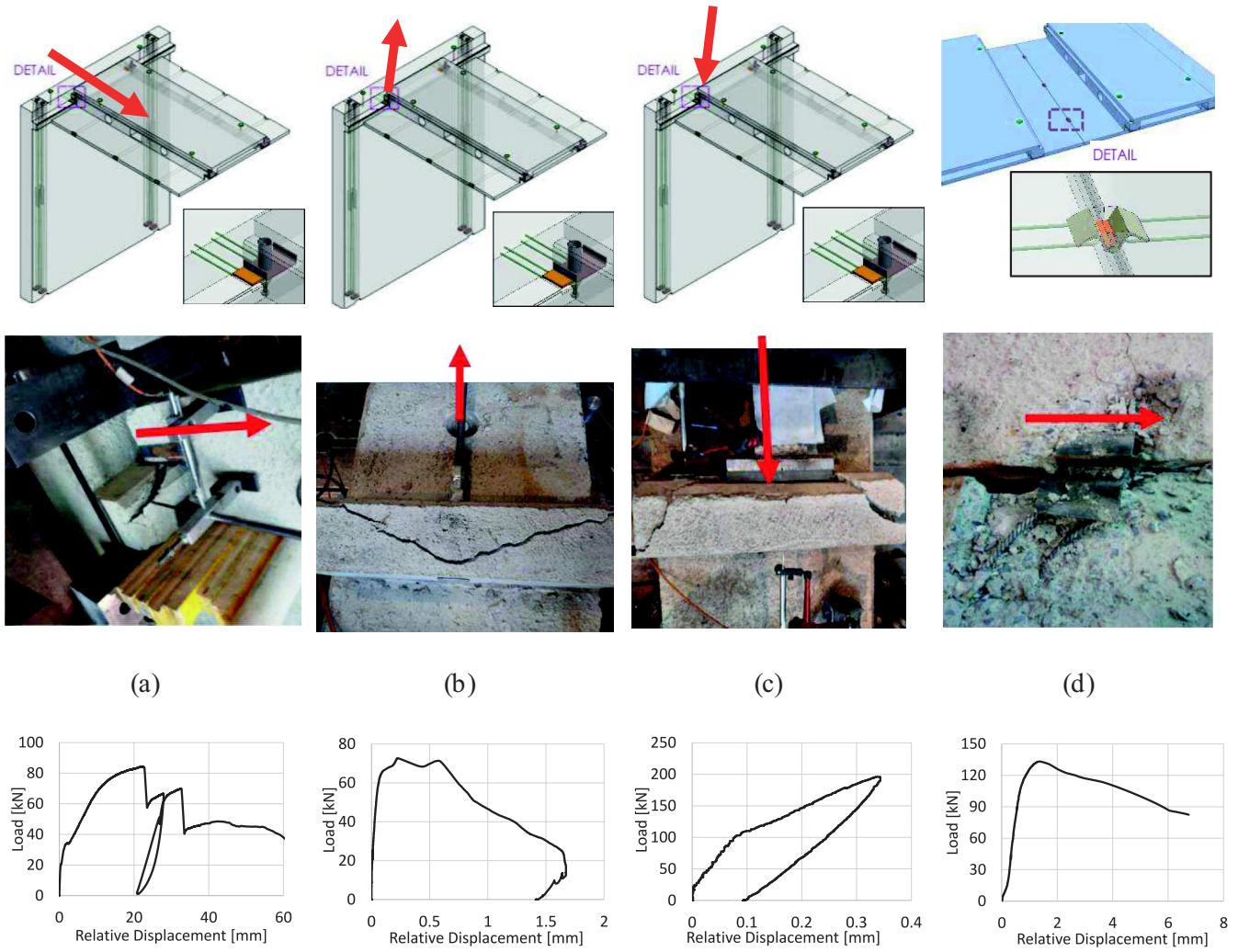

FIGURE 9 | Failure modes and results of laboratory testing of connections and joints: (a) slab dowel in shear, (b) slab dowel in tension, (c) wall/beam corbel in compression, and (d) slab-to-slab welded joint in shear.

The torque contribution of the slab is, however, not sufficient to avoid collapse whether the third wall of the portal wall is removed because this analysis did not converge due to exceedance of the lintel capacity, which also highlights that the catenary action potentially displayed by the slab elements through their dowel connections is not able to add a relevant contribution.

Concerning the notional wall removal at the lower storeys, the wall panel system was subjected to lower deflection than in the case of removal at the roof storey (as also noticeable from Figure 11b,c) due to the development of an effective frame effect in the upper wall panels ensuring full elastic behavior of both the horizontal and vertical wall elements. Convergence was found even under the extreme scenario of loss of the whole wall panel element, including the third wall portion, due to this resistance mechanism.

The frame effect displays a high horizontal compressive load in the lintel located at the storey of the wall removal and with a similar horizontal tensile load on the roof lintel, equilibrating the overturning moment of the cantilevering frame portion, whereas at all other intermediate floors, the load imposed on the transverse wall is practically only made of pure vertical shear (Figure 12). Although the compression in the lintel element immediately above the wall removed is positive for the strength under contemporary bending, the tension in the upper lintel induces a negative effect, which causes some action combinations to be very close to or slightly beyond the resistance domain (as noted by the bending moment–axial load interaction domain plotted in Figure 13a). However, an initial high tensile stress in the roof lintel, to which the frame effect is nonlinearly summed, is present in the model with wall removal at the first floor due to the unrealistic neglect of the construction stage analysis, which would most likely bring the outer points into the domain. This phenomenon suggests the use of a stronger reinforcement—or a greater number of mechanical connections with the inner transverse wall—at the roof storey joint. The positions of the load points in the interaction domain of the lintels shown in Figure 13a further confirm that the results of an elastic analysis would have been far from checked. It is also remarkable that the wall elements of the portal walls appear to be slightly stressed in all analyses, as shown in Figure 13b.

In the extreme case of removal of all three walls of the portal wall at the ground storey, the axial load of all storeys above

TABLE 3 | Main analysis results.

Precast system	Model ID [system-storey-scenario]	Max vert. displ. [mm]	Max load on wall/column			Max load on lintel/beam			Max load on slab dowel			Max load on slab weld	
			M [kNm]	V [kN]	N_c [kN]	M [kNm]	V [kN]	N_t [kN]	V [kN]	N_t [kN]	N_c [kN]	V [kN]	N [kN]
Wall	WA-34-1	5.1	228	111	281	302	143	66	51	0	45	9.1	4.9
	WA-34-12	46	225	115	622	532	256	48	17	30	90	16	25
	WA-34-123	∞	—	—	—	—	—	—	—	—	—	—	—
	WA-32-12	3.2	358	223	659	161	315	428	3	0	32	4.5	3.2
	WA-32-123	3.5	339	216	36	207	483	482	3	0	35	3.6	3.1
	WA-1-12	3.3	371	231	751	205	475	457	2	0	35	4.6	4.1
	WA-1-123	3.3	322	206	81	205	476	467	2	0	35	1.1	3.2
Coupled wall-frame	WF-34-1C	61	140	71	442	130	136	115	16	76	88	55	36
	WF-34-2C	44	107	32	411	110	123	181	18	65	66	47	35
	WF-34-1A	64	189	89	385	155	95	97	17	79	86	66	37
	WF-34-2A	60	175	75	440	189	157	134	23	90	92	73	54
	WF-32-1C	77	250	114	1387	159	196	283	18	95	110	63	50
	WF-32-2C	52	158	60	1270	114	142	317	21	75	75	52	45
	WF-32-1A	74	208	109	1217	200	177	152	19	94	102	82	60
	WF-32-2A	72	312	133	1375	200	184	369	29	105	107	85	71
	WF-1-1C	105	229	101	$1.44e^4$	174	222	466	25	135	149	93	67
	WF-1-2C	76	299	138	$1.32e^4$	118	192	560	32	102	104	62	67
	WF-1-1A	135	262	131	$1.35e^4$	200	230	172	63	92	109	148	29
	WF-1-2A	105	697	322	$1.45e^4$	207	243	677	36	144	147	114	97

Note: For the dowel connection, the axial load is with respect to the dowel bar, the longitudinal shear is in the direction of the slab element, and the transverse shear is in the direction of the beam. For the welded connection, longitudinal shear is in the axis with the welded bar (in the direction of the slab element), transverse shear is in the direction of the beam, and vertical shear is in the vertical direction orthogonal to the plane of the slab element.

FIGURE 10 | Bending moment distribution (in kNm) for the top lintel in the case of the slab: (a) not modeled (linear analysis), (b) modeled (WA-34-12), and (c) vertical torquing couples in the spaced dowel connections of the slab elements.

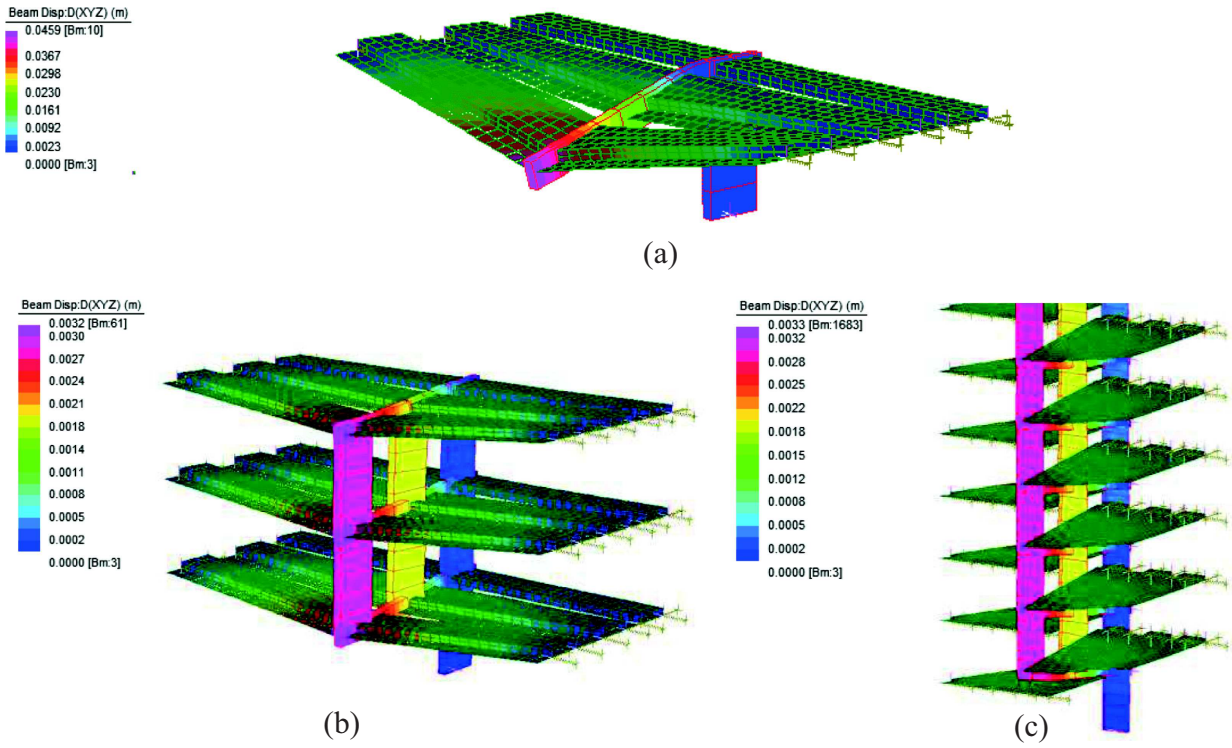

FIGURE 11 | Displacement shapes resulting from the analyses: (a) WA-34-12, (b) WA-32-12, and (c) WA-1-12.

belonging to their tributary area—evaluated at approximately 10,000 kN—follows an alternative path, as it is transmitted to the transverse wall. The transverse wall, however, is only slightly loaded under normal conditions and can bear such a strong action.

5.2 | Coupled Wall-Frame System

Considering the case study building employing the coupled wall-frame structural system, the column loss was applied in four plan locations, covering all possible relevant cases due to the double symmetry of the considered plan. Moreover, column loss scenarios were investigated for the same storeys of the wall structure previously investigated. With respect to the minimum requirements resulting from the design carried out according to static loads only, all horizontal elements (regular beams, tragolo, and special solid slab elements corresponding to the columns) that converged into a column node were made moment-resisting and provided with mechanical connections for the splicing of horizontal rebars, and their end reinforcement that converged into the joint was determined not only by the static loading but also by the column loss condition, especially the bottom reinforcement.

The results show that the loss of a single column yields nonlinear behavior of the horizontal elements directly converging into the node (including all corresponding horizontal elements above the storey where element removal occurs), whereas all other horizontal elements and all columns, including the eventual segment above the removed one, remain in the elastic field whichever is the storey at which the column is removed.

Analyzing the scenarios associated with column losses at the top storey, those encompassing the loss of a central, edge and corner column directly involve four, three, and two elements, respectively, as reflected by the displacement increase (Figure 14). It is recalled that a relevant catenary and TMA might only occur

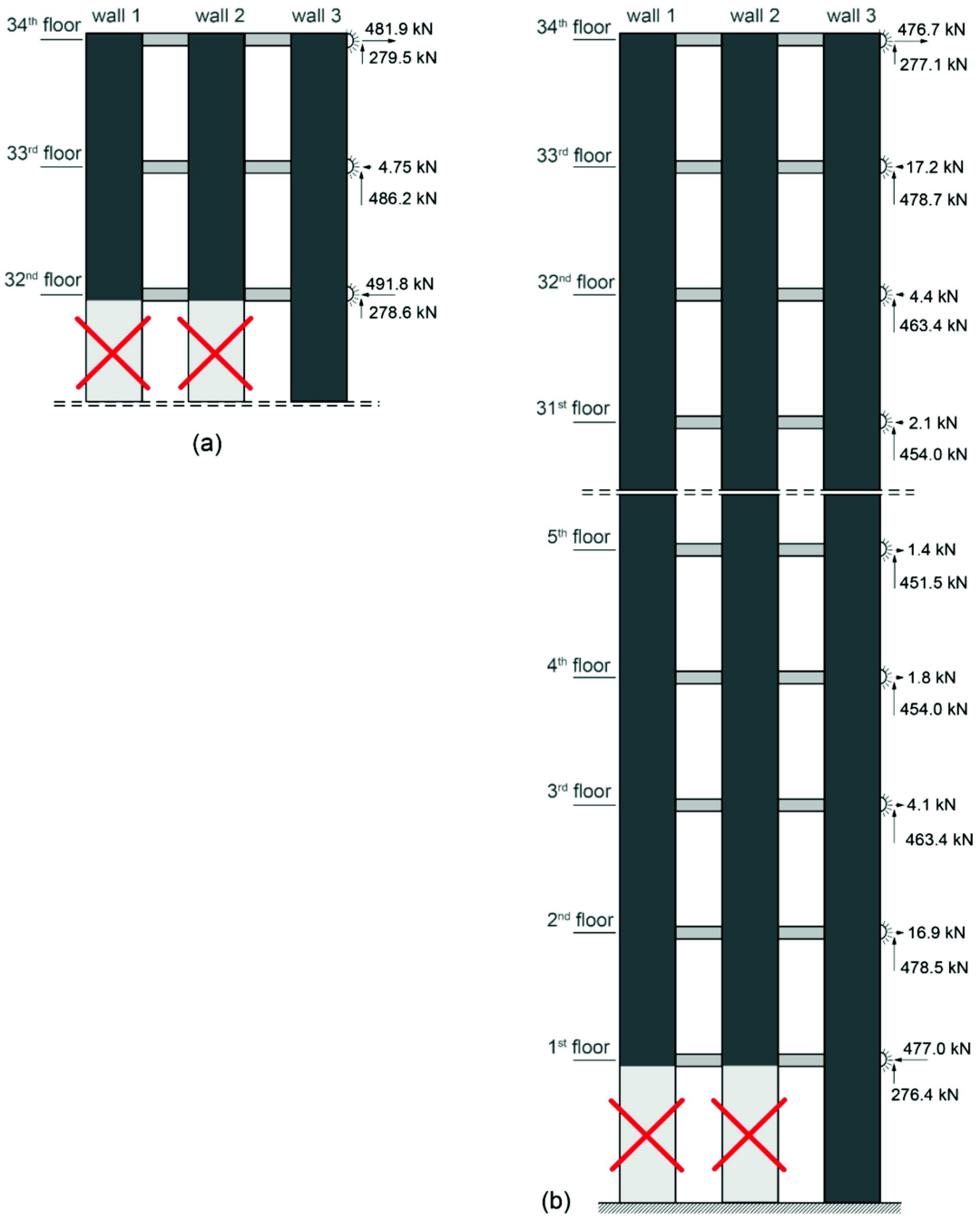

FIGURE 12 | Reactions on the transverse wall for the analyses: (a) WA-32-12 and (b) WA-1-12.

when central and edge columns are removed, respectively, although no efficient catenary/TMA can occur when corner columns are removed. Nevertheless, similar to the results obtained for the wall system, the level of displacement attained is a function of both (i) the bending resistance of the elements converging into the node where the column is removed and (ii) the torque effect ensured by the torsional stiffness of the slab elements, which allows the distanced dowel connections to mitigate the increase in the bending moment distribution in the elements due to concentrated warping couples of vertical actions (Figure 10c).

In contrast to the mechanical behavior of the wall system, greater deformation and stress in the slab elements and connections were obtained when column removal was imposed at the ground storey (Figure 15) due to the counterbalance between (a) the stiffening additional shear contribution of the horizontal elements converging into the node in the upper storeys, which is relatively weak due to their slenderness, and (b) the additional load coming from the self-weight of the column element at the upper storeys. In other words, the floor elements are too slender to form an efficient frame effect, and the lower storeys are relatively more loaded due to the weight of the columns piled directly above the one removed.

In particular, it was noted that the beam elements are too deformable to determine a crucial frame action from which the

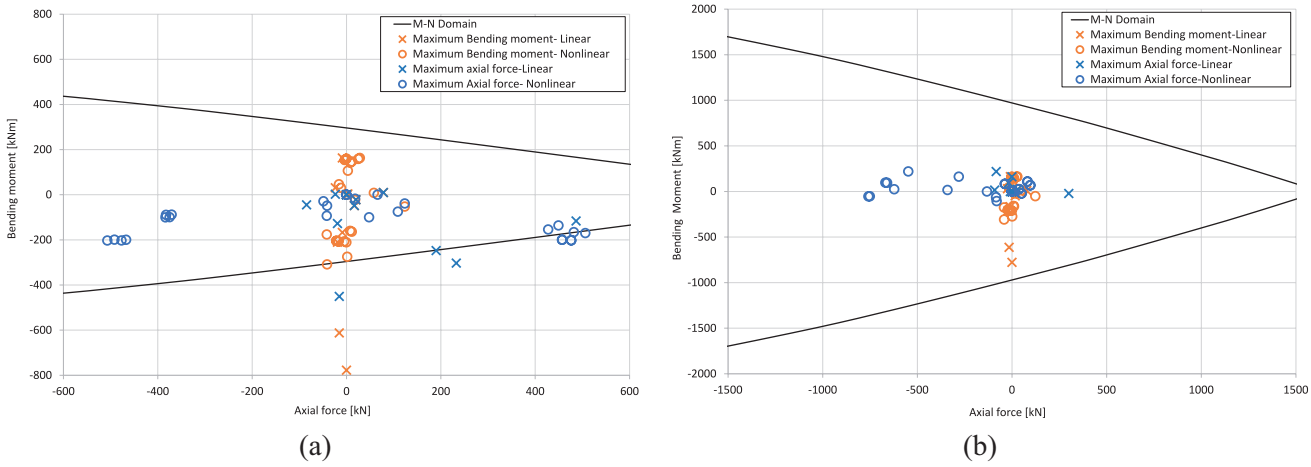

FIGURE 13 | Action combinations compared with the M-N resisting domain: (a) lintel elements and (b) wall elements.

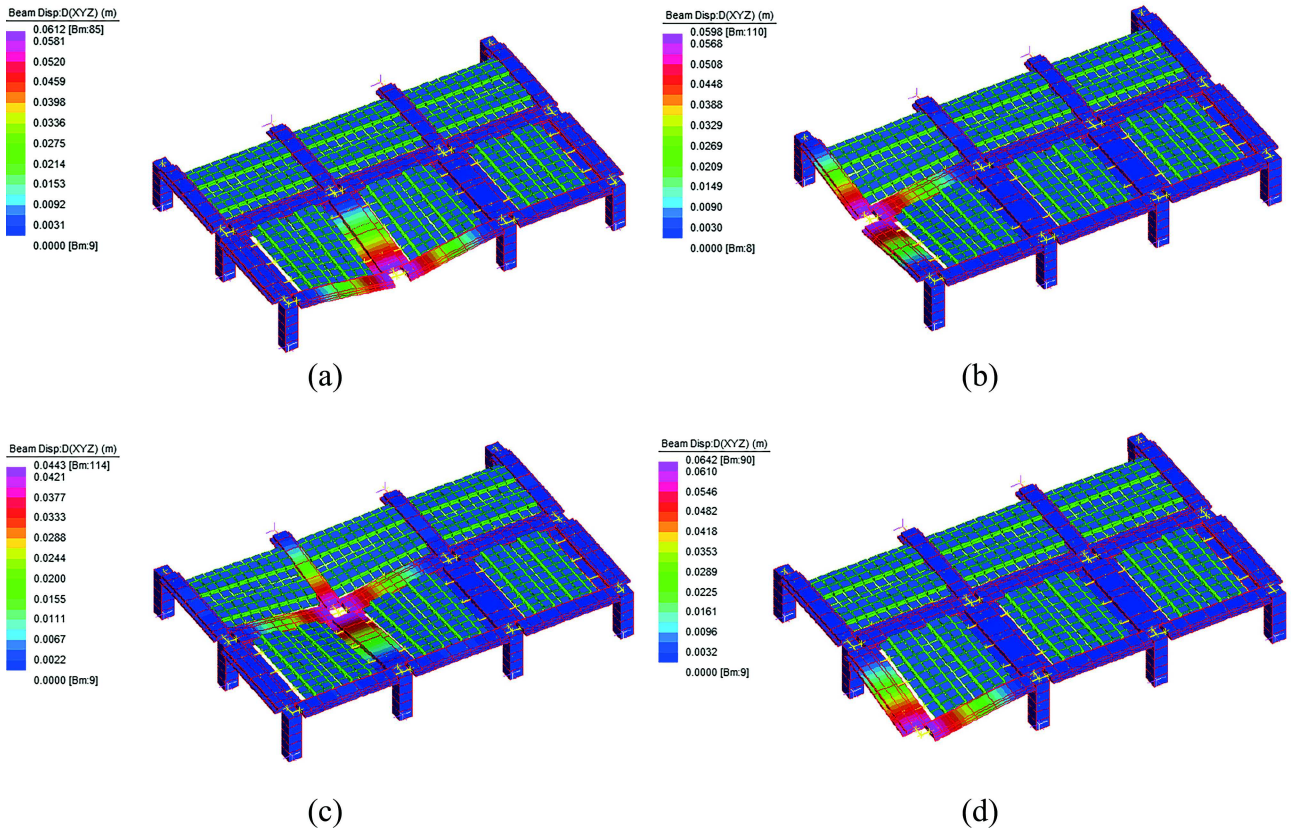

FIGURE 14 | Displacement shapes of (a) WF-34-1C, (b) WF-34-2A, (c) WF-34-2C, and (d) WF-34-1A.

robustness of the overall structural assembly would benefit, which could also reduce the end reinforcement.

As a consequence of the increase in displacement, for the central and edge columns, a contemporary increase in the tensile axial load occurs in those slab members aligned in a row and converging into the joint. However, the numerical procedure employed cannot update the moment–curvature diagrams considering the progressive changes in the axial load of the horizontal elements. A further sensitivity analysis was carried out, showing that the structure with an updated moment–curvature had reduced bending cracking and yielding strengths associated to a displacement higher by 25%, despite equilibrium could be found. A greater displacement also corresponded to a greater axial force. However, the additional axial force is a compatibility action arising from the static indeterminacy of the frame system, and it is not directly involved in the resistance mechanism. The mean inclination of the mostly stressed horizontal elements is approximately 1.5 mrad, which corresponds to a negligible vertical component of the axial force. Hence, a very slight decrease in the axial stiffness of the element in tension would cause a strong reduction in the axial force without relevant consequences for the resisting mechanism.

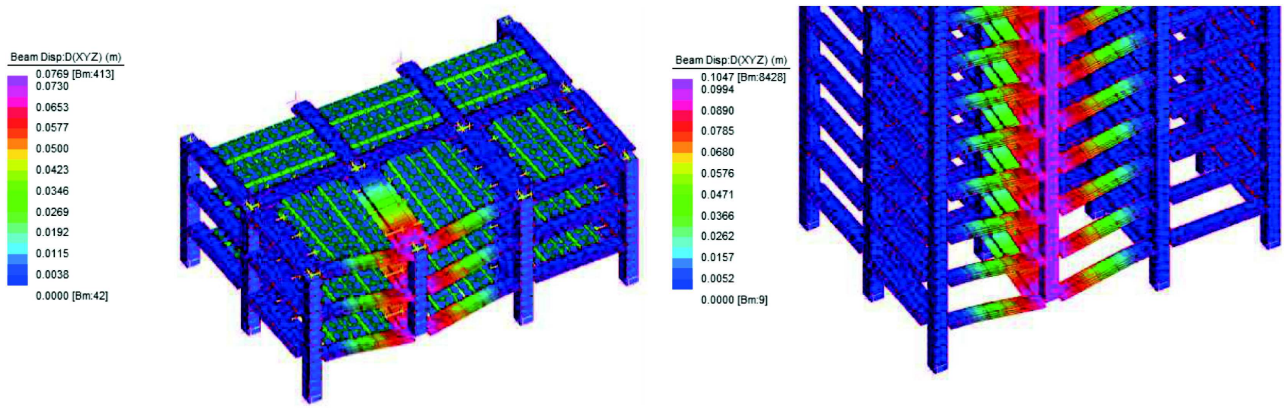

FIGURE 15 | Displacement shapes of (a) WF-32-1C and (b) WF-1-1C (slab hidden for better representation).

The current depth of all horizontal elements, equal to 0.3 m, corresponds to a reasonable minimum according to static calculations. However, increasing this depth even only for the peripheral elements (beams and tragolos), since they are the most stressed in column loss conditions, is deemed to potentially improve the formation of a more effective frame action.

6 | Conclusions

Several analyses were carried out with the aim of investigating the potential consequences of different column/wall loss scenarios in high-rise buildings designed employing modern dry-assembled precast concrete structural systems based on either wall or coupled wall-frame arrangements.

Although the work carried out is case dependent, because it considers specific case study buildings employing specific precast structural systems, the methodology employed and its findings are deemed to be of general interest and to provide design hints useful to both guide the conception of designers and provide them with instruments for detailed checks.

Two resistance mechanisms—(1) the frame action of the elements above the removed column acting in bending/shear and (2) the torque action of the slab system displayed through warp coupling of vertical actions in the dowel connections installed in the ribs—work in parallel and are independent sources of structural robustness for both considered precast systems. The frame effect becomes predominant only for the wall panel system when column loss occurs below the roof storey, mainly due to the large depth of the beam lintel element, whereas the combination of both effects is always effective in ensuring robustness in the frame system. The two systems provide opposite trends when moving the removal of a primary element to lower storeys: The maximum deformation decreases for the wall system due to the activation of the frame behavior above, although it increases for the coupled wall-frame system due to the progressive increase in load induced by the self-weight of the column above, where the frame action mainly occurs in plane in the horizontal members converging in the joint, without effectively involving the columns.

As a consequence of the frame effect arising in the wall system when removal of a primary element is carried out at a storey lower than the top, a dangerous concentration of strong tensile load is displayed at this single roof joint between transverse walls, which suggests employing stronger reinforcement or a greater number of connectors in this location.

The slab connections are fundamental for providing a rigid diaphragm effect that conveys spurious lateral forces from the finding of ALP to the stiffer elements of the building, as well as ensuring the beneficial behavior of the slab system in combined multiaxial bending and torque. Indeed, the actions on the connections appear in all the analyzed cases to be compatible with the strength and mechanical behavior associated with slab-to-beam dowel and slab-to-slab welded connections after experimental calibration, even if they appear to be stressed by complex multiaxial interactions of forces, which may inspire further experimentation. In particular, the torsional effect of the slab is due to the couple of vertical actions displayed in the dowel connections corresponding to the ribs combined with the downward gravity components and shear in both horizontal directions, and triaxial loads are applied to the welded slab-to-slab connections.

The displacements obtained in the analyses, of the order of a few centimeters in the worse cases, are much smaller in comparison with those traditionally associated with large displacement second-order effects such as catenary action, thus making the studied precast wall system much less vulnerable (and more easily repairable) than more traditional cast-in-situ and precast RC systems under the scenario of loss of primary elements.

From the results of the nonlinear static analyses, it can be concluded that both the precast systems investigated offer relevant structural robustness in the case of loss of either single or multiple primary load-bearing elements when they are designed for this purpose, taking advantage of the specific peculiarities of dry-assembled precast systems that avoid concrete pouring in the whole superstructure, despite deviations from the general indications related to other more standard typologies of cast-in-situ and precast RC systems with wet joints. This finding is deemed to also inspire future code evolutions.

Acknowledgments

The company Brusnika L.l.c. is kindly acknowledged for the support. Open access publishing facilitated by Universita degli Studi dell'Insubria, as part of the Wiley - CRUI-CARE agreement.

Conflicts of Interest

The first author is partner of DLC Consulting srl of Milan, Italy, which is a structural engineering consultant company active in different fields, which include precast concrete structures, the main subject of the presented research. The analyzed precast structural systems were conceived by the consultant. During the development of the work, the second author was a collaborator of the same consultant. The third author declares no conflicts of interest. The authors, however, do not recognize explicit possible benefits to the financial/commercial activity of the above consultant from the possible dissemination of the paper, which maintains a strict scientific approach aimed at filling the gap of the knowledge of the specific field of the study.

Data Availability Statement

The data that support the findings of this study are available from the corresponding author upon reasonable request.

References

1. B. R. Ellingwood and D. O. Dusenberry, "Building Design for Abnormal Loads and Progressive Collapse," *Computer-Aided Civil and Infrastructure Engineering* 20, no. 3 (2005): 194–205.

2. C. Brett and Y. Lu, "Assessment of Robustness of Structures: Current State of Research," *Frontiers of Structural and Civil Engineering* 7, no. 4 (2013): 356–368.

3. J. M. Adam, F. Parisi, J. Sagaseta, and X. Lu, "Research and Practice on Progressive Collapse and Robustness of Building Structures in the 21st Century," *Engineering Structures* 173 (2018): 122–149.

4. X. Lu, H. Guan, H. Sun, et al., "A Preliminary Analysis and Discussion of the Condominium Building Collapse in Surfside, Florida, US, June 24, 2021," *Frontiers of Structural and Civil Engineering* 15 (2021): 1097–1110.

5. H. J. Yallop, "The Pressures Developed in the Ronan Point Explosion," *Journal of the Forensic Science Society* 9, no. 1 (1969): 45–47.

6. C. Pearson and N. Delatte, "Ronan Point Apartment Tower Collapse and Its Effect on Building Codes," *Journal of Performance of Constructed Facilities* 19, no. 2 (2005): 172–177.

7. J. M. Russell, J. Sagaseta, D. Cormie, and A. E. K. Jones, "Historical Review of Prescriptive Design Rules for Robustness After the Collapse of Ronan Point," *Structure* 20 (2019): 365–373.

8. E. Romano, O. Iuorio, and N. Nikitas, P. Negro, "A Review on Retrofit Strategies for Large Panel System Buildings," in *Proceedings of the Sixth International Symposium on Life-Cycle Civil Engineering* (IALCCE2018) (Ghent, Belgium, 2019), 3023–3030.

9. S. Matthews and B. Reeves, "Large Panel System Dwelling Blocks – Updating Structural Assessment Guidance," *Proceedings of the Institution of Civil Engineers: Forensic Engineering* 165, no. 1 (2012): 21–37.

10. Ł. Ślaga, "Catenary Action in Precast Skeleton Structures - Protection Agains Progressive Collapse," in *Proc. JUNIORSTAV2013* (Brno, Czech Republic, 2013).

11. D. Gouverneur, R. Caspeele, and L. Taerwe, "Experimental Investigation of the Load–Displacement Behaviour Under Catenary Action in a Restrained Reinforced Concrete Slab Strip," *Engineering Structures* 49 (2013): 1007–1016.

12. J. Yu and K. H. Tan, "Structural Behavior of RC Beam-Column Subassemblages Under a Middle Column Removal Scenario," *ASCE Journal of Structural Engineering* 139, no. 2 (2013): 233–250.

13. H. S. Lew, Y. Bao, S. Pujol, and M. A. Sozen, "Experimental Study of Reinforced Concrete Assemblies Under a Column Removal Scenario," *ACI Structural Journal* 111, no. 4 (2014): 881–892.

14. F. Palmisano, "Mitigation of Progressive Collapse by the Activation of the Elasto-Plastic Catenary Behaviour of R.C. Slab Structures," *Open Construction and Building Technology Journal* 8 (2014): 122–131.

15. N. S. Lim, K. H. Tan, and C. K. Lee, "Effects of Rotational Capacity and Horizontal Restraint on Development of Catenary Action in 2-D RC Frames," *Engineering Structures* 153 (2017): 613–627.

16. X. Lu, K. Lin, Y. Li, H. Guan, P. Ren, and Y. Zhou, "Experimental Investigation of RC Beam-Slab Substructures Against Progressive Collapse Subject to an Edge-Column-Removal Scenario," *Engineering Structures* 149 (2017): 91–103.

17. L. T. Deputy, Y. Zeinali, and B. A. Story, "A Modified Catenary Model With Application to the Analysis and Design of Retrofit Cables for Progressive Collapse," *Infrastructures* 3, no. 320 (2018): 26.

18. A. T. Pham and K. H. Tan, "Static and Dynamic Responses of Reinforced Concrete Structures Under Sudden Column Removal Scenario Subjected to Distributed Loading," *ASCE Journal of Structural Engineering* 145, no. 1 (2019): 04018235.

19. H. M. Elsanadedy, Y. A. Al-Salloum, T. H. Almusallam, T. Ngo, and H. Abbas, "Assessment of Progressive Collapse Potential of Special Moment Resisting RC Frames – Experimental and FE Study," *Engineering Failure Analysis* 105 (2019): 896–918.

20. I. M. H. Alshaikh, B. H. A. Bakar, E. A. H. Alwesabi, and H. M. Akil, "Experimental Investigation of the Progressive Collapse of Reinforced Concrete Structures: An Overview," *Structure* 25 (2020): 881–900.

21. M. Colombo, P. Martinelli, and M. di Prisco, "A Design Approach to Evaluate the Load-Carrying Capacity of Reinforced Concrete Slabs Considering Tensile Membrane Action," *Structural Engineering International* 31, no. 2 (2021): 260–270.

22. P. Martinelli, M. Colombo, S. Ravasini, and B. Belletti, "Application of an Analytical Method for the Design for Robustness of RC Flat Slab Buildings," *Engineering Structures* 258 (2022): 114117.

23. J. Yu, L. Z. Luo, and Q. Fang, "Structure Behavior of Reinforced Concrete Beam-Slab Assemblies Subjected to Perimeter Middle Column Removal Scenario," *Engineering Structures* 208 (2020): 110336.

24. T. H. Almusallam, H. M. Elsanadedy, Y. A. Al-Salloum, N. A. Siddiqui, and R. A. Iqbal, "Experimental Investigation on Vulnerability of Precast RC Beam-Column Joints to Progressive Collapse," *KSCE Journal of Civil Engineering* 22, no. 10 (2018): 3995–4010.

25. M. Scalvenzi, S. Ravasini, E. Brunesi, and F. Parisi, "Progressive Collapse Fragility of Substandard and Earthquake-Resistant Precast RC Buildings," *Engineering Structures* 275 (2023): 115242.

26. H. M. Elsanadedy, T. H. Almusallam, Y. A. Al-Salloum, and H. Abbas, "Investigation of Precast RC Beam-Column Assemblies Under Column-Loss Scenario," *Construction and Building Materials* 142 (2017): 552–571.

27. F. F. Feng, H. J. Hwang, and W. J. Yi, "Static and Dynamic Loading Tests for Precast Concrete Moment Frames Under Progressive Collapse," *Engineering Structures* 213 (2020): 110612.

28. K. Qian and B. Li, "Investigation into Precast Concrete Floors against Progressive Collapse," *ACI Structural Journal* 162, no. 2 (2019): 171–182.

29. S. Ravasini, B. Belletti, E. Brunesi, R. Nascimbene, and F. Parisi, "Nonlinear Dynamic Response of a Precast Concrete Building to Sudden Column Removal," *Applied Sciences* 11 (2021): 599.

30. F. Wang, J. Yang, and S. Shah, "Effect of Horizontal Restraints on Progressive Collapse Resistance of Precast Concrete Beam-Column

Framed Substructures," *KSCE Journal of Civil Engineering* 24, no. 3 (2020): 879–889.

31. Y. Zhou, T. Chen, Y. Pei, et al., "Static Load Test on Progressive Collapse Resistance of Fully Assembled Precast Concrete Frame Structure," *Engineering Structures* 200 (2019): 109719.

32. Y. Zhou, X. Hu, Y. Pei, et al., "Dynamic Load Test on Progressive Collapse Resistance of Fully Assembled Precast Concrete Frame Structures," *Engineering Structures* 214 (2020): 110675.

33. D. D. Joshi and P. V. Patel, "Experimental Study of Precast Dry Connections Constructed Away From Beam–Column Junction Under Progressive Collapse Scenario," *Asian Journal of Civil Engineering* 20, no. 2 (2019): 209–222.

34. D. C. Feng, Z. Wang, and G. Wu, "Progressive Collapse Performance Analysis of Precast Reinforced Concrete Structures," *Structural Design of Tall and Special Buildings* 28, no. 5 (2019): e1588.

35. M. Buitrago, N. Makoond, J. J. Moragues, J. Sagaseta, and J. M. Adam, "Robustness of a Full-Scale Precast Building Structure Subjected to Corner-Column Failure," *Structure* 52 (2023): 824–841.

36. D. C. Feng, M. X. Zhang, E. Brunesi, F. Parisi, J. Yu, and Z. Zhou, "Investigation of 3D Effects on Dynamic Progressive Collapse Resistance of RC Structures Considering Slabs and Infill Walls," *Journal of Building Engineering* 54 (2022): 104421.

37. D. C. Feng, H. R. Shi, E. Brunesi, F. Parisi, and C. L. Wang, "Efficient Numerical Model for Progressive Collapse Analysis of Prestressed Concrete Frame Structures," *Engineering Failure Analysis* 129 (2021): 105683.

38. B. Dal Lago and A. Dal Lago, "New Precast Constructions for Integrated Complex Urban Interventions," *BFT International* 84, no. 4 (2018): 72–80.

39. B. Dal Lago, S. Bianchi, and F. Biondini, "Diaphragm Effectiveness of Precast Concrete Structures With Cladding Panels Under Seismic Action," *Bulletin of Earthquake Engineering* 17, no. 1 (2019): 473–495.

40. B. Dal Lago and L. Ferrara, "Efficacy of Roof-To-Beam Mechanical Connections on the Diaphragm Behaviour of Precast Decks With Spaced Roof Elements," *Engineering Structures* 176 (2018): 681–696.

41. B. Dal Lago and K. Gajera, "Progressive Collapse Prevention in High-Rise Precast Wall Buildings With Prestressed Voided Floor Elements Assembled With Mechanical Connections," in *fib Symposium 2021* (Lisbon, Portugal, 2021), 1081–1090.

42. K. Lin, X. Lu, Y. Li, and H. Guand, "Experimental Study of a Novel Multi-hazard Resistant Prefabricated Concrete Frame Structure," *Soil Dynamics and Earthquake Engineering* 119 (2019): 390–407.

43. S. E. Quiel, C. J. Naito, and C. T. Fallon, "A Non-emulative Moment Connection for Progressive Collapse Resistance in Precast Concrete Building Frames," *Engineering Structures* 179 (2019): 174–188.

44. B. Dal Lago, M. Muhaxheri, and L. Ferrara, "Numerical and Experimental Analysis of an Innovative Lightweight Precast Concrete Wall," *Engineering Structures* 137 (2017): 204–222.

45. P. Negro, D. A. Bournas, and F. J. Molina, "Pseudodynamic Tests on a Full-Scale 3-Storey Precast Concrete Building: Global Response," *Engineering Structures* 57 (2013): 594–608.

46. F. Foti and B. Dal Lago, "Mitigation of Wind-Induced Vibrations in High-Rise Dry-Assembled Precast Concrete Residential Tower Buildings," in *10th UBT IC-CEIE* (Pristina, Kosovo, 2021), Paper No. 301.

47. M. Muhaxheri and B. Dal Lago, "Local Modelling of Cast-In Threaded Dowel Bar Connections of Precast Joints Under Lateral Loading," in *18WCEE* (Milan, Italy, 2024).

48. B. Dal Lago, M. Del Galdo, and D. Bisi, "Tests and Design of Welded-Bar Angle Connections of Precast Floor Elements," *Journal of Advanced Concrete Technology* 20, no. 2 (2022): 43–56.

49. B. Dal Lago, D. Bisi, M. Del Galdo, A. Dal Lago, G. Muciaccia, and L. Ferrara, "Experimentation and Design Rules of Loop-Reinforced Diamond-Shaped Joints for Load-Bearing Precast Concrete Walls," in *Italian Concrete Days 2020* (Naples, Italy, 2021).

50. B. Dal Lago, M. Del Galdo, E. Papa, and A. Dal Lago, "Tests on Ductile Short-Length Splice Connections for Precast Concrete Load-Bearing Elements," in *fib Symposium 2021* (Lisbon, Portugal, 2021), 1109–1118.

51. B. Dal Lago, G. Toniolo, and M. Lamperti Tornaghi, "Influence of Different Mechanical Column-Foundation Connection Devices on the Seismic Behaviour of Precast Structures," *Bulletin of Earthquake Engineering* 14, no. 12 (2016): 3485–3508.

52. "EN 1991-1-7, Eurocode 1 - Action on Structures - Part 1–7: General Actions - Accidental Actions," European Committee for Standardisation (2006).

53. fib, *Bulletin 63: Design of Precast Concrete Structures Against Accidental Actions* (Lausanne, Switzerland: Fédération Internationale du Béton/International Association for Structural Concrete, 2012).

54. D. Cormie, *Manual for the Systematic Risk Assessment of High-Risk Structures Against Disproportioned Collapse* (London, UK: The Institution of Structural Engineers, 2013).

55. S. Matthews, A. Bigaj-van Vliet, J. Walraven, G. Mancini, and G. Dieteren, *fib, Model Code for Concrete Structures 2020* (Lausanne, Switzerland: Fédération Internationale du Béton - International Federation for Concrete, 2023).

56. F. Biondini and D. M. Frangopol, "Time-Variant Robustness of Aging Structures," in *Maintenance and Safety of Ageing Infrastructure*. Structures and Infrastructures Book Series, vol. 10, eds. Y. Tsompanakis and D. M. Frangopol (Boca Raton, FL, USA: CRC Press, Taylor & Francis, 2014), 163–200.

57. F. Biondini and S. Restelli, "Damage Propagation and Structural Robustness," in *IALCCE08*, eds. F. Biondini and D. M. Frangopol (Varenna, Italy: CRC Press, Taylor and Francis, 2008).

58. G+D Computing, "Using Strand7 (Straus7) – Introduction to the Strand7 Finite Element Analysis System. Ed. 3," (Sydney, Australia: Strand7 Pty Limited, 2010).

59. fib, *Model Code for Concrete Structures 2010* (Lausanne, Switzerland: Fédération Internationale du Béton - International Federation for Concrete, 2013).

60. D. A. Bournas, P. Negro, and F. J. Molina, "Pseudodynamic Tests on a Full-Scale 3-Storey Precast Concrete Building: Behavior of the Mechanical Connections and Floor Diaphragms," *Engineering Structures* 57 (2013): 609–627.

61. F. Stochino, "RC Beams Under Blast Load: Reliability and Sensitivity Analysis," *Engineering Failure Analysis* 66 (2016): 544–565.